Energetic Particle Mode Dynamics in Tokamaks

F. Zonca, S. Briguglio, L. Chen†, G. Fogaccia, G. Vlad, and L.-J. Zheng†

ENEA C. R. Frascati, C.P. 65, 00044 Frascati, Rome, Italy
† Department of Physics and Astronomy, University of California, Irvine, CA 92717-4575

E-mail contact of main author: zonca@frascati.enea.it

Abstract. Energetic Particle Modes [1] (EPM) are *strongly driven oscillations* excited via wave-particle resonant interactions at the characteristic frequencies of the energetic ions [1, 2], ω_{tE}, ω_{BE} and/or $\overline{\omega}_{dE}$, *i.e.*, respectively the transit frequency for circulating particles and the bounce and precessional drift frequencies for trapped ions. A sharp transition in the plasma stability at the critical EPM excitation threshold has been observed by *nonperturbative* gyrokinetic codes in terms of changes in normalized growth rate (γ/ω_A, with $\omega_A = v_A/qR_0$), real frequency (ω_r/ω_A) and parallel wave vector ($k_\parallel qR_0$) both as $\alpha = -R_0q^2\beta'$ [3, 4] of the thermal plasma and that, α_E [3, 5, 6], of fast ions are varied. The present work further explores theoretical aspects of EPM excitations by spatially localized particle sources, possibly associated with frequency chirping, which can *radially trap* the EPM in the region where the free energy source is strongest. Results of a *nonperturbative* 3D Hybrid MHD Gyrokinetic code [5] are also presented to emphasize that nonlinear behaviors of EPM's are different from those of Toroidal Alfvén Eigenmodes (TAE) [7] and Kinetic TAE (KTAE) [8] and that particle losses and mode saturation are consistent with the *mode-particle pumping* model [9] (*particle radial convection*). Results of theoretical analyses of nonlinear EPM dynamics are also presented and the possible overlap with more general nonlinear dynamics problems is discussed.

1. EPM Excited by Ion Cyclotron Radio Frequency (ICRF) Heating.

A one-dimensional fast particle simulation code (FAPS-1D) has been developed to study the trapped energetic particle effects on the short wavelength (high toroidal mode number n) Alfvénic modes in the tokamak configuration. The code employs the gyrokinetic (GKE) - magnetohydrodynamic (MHD) hybrid simulation scheme. Thus, the core plasma is described by the MHD fluid equations, while the energetic particle species are described by the linearized GKE equations. This allows us to study in detail the kinetic effects of the energetic particles, such as wave-particle resonance and finite orbit size effects. The MHD fluid (or vorticity) equation is solved via a predictor - corrector algorithm. The GKE equation for the energetic particles is solved by a δf particle-in-cell simulation method. Specially, simulations are performed to study the interactions between the Alfvén modes and the trapped energetic ions produced by the ICRF heating [3].

It is found that for the trapped energetic ions the wave-particle resonances are mainly due to the precessional drift resonance, as indicated by the fact that the real part of the mode frequency $\Omega_r = \omega_r/\omega_A$ increases with $k_\theta\rho_A$, $\rho_A = v_A/\omega_{cE}$, for small $k_\theta\rho_A$. This is further confirmed by examining the phase diagram of the averaged nonadiabatic distribution function, $\sum g_i$, which shows that there are two resonances (180-degree-phase shift): one peaks at a lower resonance energy (normalized to the effective ICRF tail ion thermal energy) $E^l_{rs} \approx 0.75$ and the other has a higher value, $E^h_{rs} \approx 3$. It can be demonstrated that the lower one corresponds to the bounce resonance, while the higher one to the precessional drift resonance.

Both the TAEs and energetic particle modes (EPMs) are found to be excited by the trapped energetic particles. Transitions between various modes are observed in the simulations, as shown

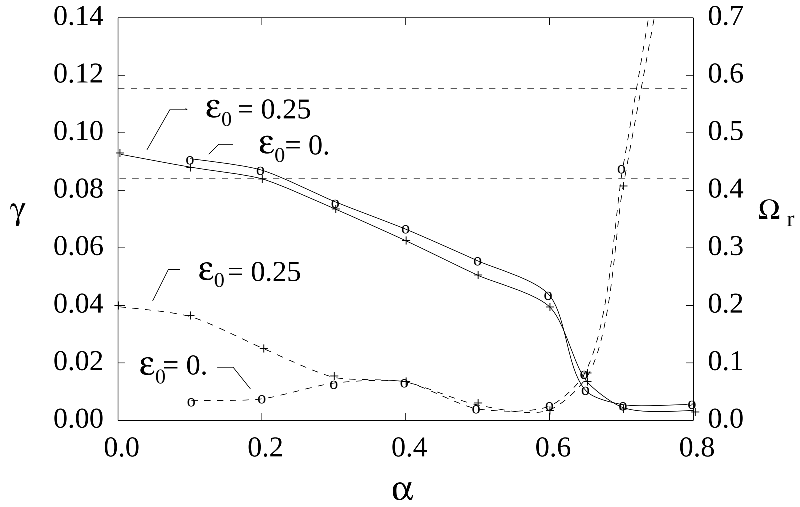

FIG. 1. : Growth rate (dashed curve) and real frequency (solid curve) vs α. Cases with $\epsilon_0 = 0$ and $\epsilon_0 = 0.25$ are denoted, respectively, by "o" and "$+$".

in FIG. 1. When α (the normalized beta value) is low, Ω_r is located in the gap and TAE dominates. As α increases, Ω_r shifts downward into the lower continuum and the mode transforms into an EPM. When α is increased further, the ballooning instability limit is reached. Ω_r then approaches to zero and the growth rate increases appreciably. To further demonstrate the effect of the continuum damping, we have also plotted in FIG. 1 the case with $\epsilon_0 \equiv 2(r/R_0 + \Delta') = 0$, i.e., with the TAE frequency gap being intentionally turned off. Note that Ω_r for both $\epsilon_0 = 0$ and $\epsilon_0 = 0.25$ (finite TAE frequency gap) are approximately the same; while $\gamma = \mathbb{Im}(\omega/\omega_A)$ of the $\epsilon_0 = 0$ case is much more reduced than that of the $\epsilon_0 = 0.25$ case. Note that, for $\epsilon_0 = 0$, there is no TAE gap and, hence, the continuum damping is always finite; in contrast to the $\epsilon_0 = 0.25$ case where Ω_r resides inside the gap and there is negligible continuum damping.

Sharp transitions in the plasma stability at the critical EPM excitation threshold, similar to those discussed here, have been observed by *nonperturbative* gyrokinetic codes in terms of changes in normalized growth rate (γ/ω_A), real frequency (ω_r/ω_A) and parallel wave vector ($k_\parallel q R_0$) both as α [3, 4] and α_E [3, 5, 6] are varied. These strong dependencies of both EPM frequency and growth rate on thermal plasma as well as energetic particle pressure profiles are in good agreement with the experimental observations of Beta induced Alfvén Eigenmodes (BAE) [10] and also suggest another explanation [3] for the existence of *frequency chirping* modes observed in most large tokamaks. In a recent work [11], theoretical aspects of EPM excitations by spatially localized particle sources, possibly associated with frequency chirping, were further explored. There, it was demonstrated that, when the characteristic scale length of the fast particle pressure profile becomes shorter than the typical separation between rational surfaces, the steep gradient can *radially trap* the EPM in the region where the free energy source is strongest, at the same time minimizing continuum damping [11]. This result yields a particularly low threshold for EPM excitation in low magnetic shear regions.

2. Modulational Instability of EPM

Results of a *nonperturbative* 3D Hybrid MHD Gyrokinetic code [5] are presented in this Section in order to emphasize that nonlinear behaviors of EPMs are different from those of TAE and KTAE. In particular, we confirm previous findings that strong radial redistributions in the energetic particle source take place when the EPM excitation threshold is exceeded, yielding potentially large particle losses and, eventually, mode saturation. Such a threshold may occur at experimentally accessible values of β_E, *e.g.*, as low as $\beta_{E0} = 0.75\%$ (on axis value) for $n = 8$ EPM excitation with $\rho_A/a = 0.01$ and a pressure profile, $\beta_E = \beta_{E0}\exp(-r^2/L_{pE}^2)$, with $L_{pE}/R_0 \simeq 0.075$ [12]. With the same parameters and profiles, FIG. 2 shows new simulation results which illustrate the nonlinear dynamic evolution of an $n = 8$ EPM. After the first phase in which the eigenmode structure forms (up to $t = 36R_0/v_A$, FIG. 2A), it appears clearly - from the modifications in the fast ion line density - that strong particle redistributions take place from $t = 36R_0/v_A$ (FIG. 2A) up to $t = 72R_0/v_A$ (FIG. 2B), which are consistent with the *mode-particle pumping* model [9] (*particle radial convection*). However, while it was shown that these nonlinear dynamics dominate particle losses and mode saturation al low-n above the EPM excitation threshold [5, 12], FIG. 2 indicates a new dynamical process that becomes important for nonlinear EPM evolution already at moderate n. Evident radial fragmentation of the EPM coherent eddies ($k_\theta = k_\parallel = 0$, $k_r \neq 0$) is present in FIG. 2B, and it is visible both in the contour-plots and in the radial variation of the various poloidal harmonics in which the eigenmode is decomposed. This fragmentation, meanwhile, is associated with a diffusive transport of fast ions, as it may be inferred from modifications in the fast particle density profile up to $t = 144R_0/v_A$ (FIG. 2C).

The *radial fragmentation* of EPM coherent eddies has a clear analogy and possible overlaps with more general nonlinear dynamics problems, and specifically with the spontaneous excitation of *zonal flows* by drift-Alfvén turbulence [13]. Within this framework, we have recently demonstrated that EPM may yield to *spontaneous excitation of zonal flows* since they are modulationally unstable above a given amplitude threshold of the coherent eddies which they form above their excitation threshold. The EPM nonlinear (NL) evolution is dominated by fast ions nonlinearities (which enter in the ballooning interchange term in the vorticity equation [13]) for $(\alpha_E/\beta_i)(R_0/r)^{1/2}(T_i/T_E)\epsilon_0^{-1} \gg 1$, which is typical for unstable EPMs. Meanwhile, fast ions nonlinearities play a role via NL modifications of their nonadiabatic response, $\delta\overline{H}_k \sim (\delta\phi - v_\parallel\delta A_\parallel/c)_{k'}\delta\overline{H}_{\rm z}$, where k, k' subscripts refer to the high frequency EPMs and sidebands, generated via NL interaction with the low frequency zonal field (subscript z). Thus, the NL fast ion response is formally equivalent to a *quasi-linear diffusion*, consistently with numerical simulations. In general, it is possible to show (details will be given elsewhere [14]) that the NL growth rate, $\Gamma_{\rm z}$, of the EPM driven zonal flow associated with $\delta\phi_{\rm z}$ is given by

$$\begin{aligned}
\Gamma_{\rm z} &= \left(\frac{9}{8|\partial D_I/\partial\omega_r|}\right)^{1/3}\gamma_M^{2/3} \quad , \\
\gamma_M^2 &= \pi\epsilon_0\frac{v_E^2}{v_A^2}\frac{\beta_E q^2}{8}q^2k_\theta^4\rho_{LE}^4k_{\rm z}^2v_E^2\left|\frac{e_EA_0}{T_E}\right|^2\sum_\ell\sum_{\sigma=\pm}\left(|\Omega_r^2-1/4|+\sigma|\Lambda|\right)\left\langle\frac{F_{0E}}{n_{0E}}\left(\frac{\hat{\omega}_{*E}}{\omega_r}-1\right)\right. \\
&\left.\delta(\mathcal{L}_{\ell,\sigma}/\omega_r)\left\langle\left\langle J_0^2(\lambda_L)\frac{\ell^2J_\ell^2(\lambda_d)}{\lambda_d^2}\right\rangle\right\rangle^2 J_0^2(\lambda_{\rm z})\left(\frac{v_\perp^2}{2v_E^2}+\frac{v_\parallel^2}{v_E^2}\right)^4\right\rangle \quad . \qquad (1)
\end{aligned}$$

Here, $D_{R,I}$ are the real and imaginary parts of the EPM linear dispersion function, $v_E^2 = T_E/m_E$, $k_{\rm z}$ is the radial wave-vector of $\delta\phi_{\rm z}$, A_0 is the amplitude of EPM scalar potential fluctuations, $\hat{\omega}_{*E} = \omega_{*nE} + \omega_{*TE}[(v_\parallel^2+v_\perp^2)/2v_E^2 - 3/2]$ for Maxwellian fast ions, Λ is the strength of continuum damping, $\mathcal{L}_{\ell,\sigma} = (v_\parallel/qR_0)(\ell+\Lambda+\sigma/2)-\omega$ is the linear EPM propagator, λ_L contains finite Larmor orbit effects, λ_d those of finite drift orbit width, and $\lambda_{\rm z} = (k_{\rm z}/k_\perp)\lambda_d$. Meanwhile, $< \ldots >$ and $<< \ldots >>$ indicate, respectively, integration in velocity and ballooning spaces. It may be shown that $\gamma_M^2 \sim \epsilon_0\alpha_E|k_\theta\rho_{LE}|k_{\rm z}^2v_A^2|\delta B_\theta/B|^2$. Thus, Eq. (1) gives a $\Gamma_{\rm z} \propto |\delta B_\theta/B|^{2/3}$ scaling. The zonal flow generation by EPM is also accompanied by a NL frequency shift $\Delta_z = \pm\Gamma_z/\sqrt{3}$. Since Eq. (1) assumes $\Gamma_z \gg |\Delta_L|$, with

$$\Delta_L = (nq')^2 \frac{\partial^2 D_R/\partial k_r^2}{\partial D_R/\partial \omega_r} \left[1 - \cos\left(\frac{k_z}{nq'}\right)\right] \quad ,$$

it is evident that there is a finite amplitude threshold to overcome for the zonal flow excitation and for radial fragmentation of the EPM coherent eddies to set in. Further analyses are in progress to quantitatively compare our theoretical estimates of Γ_z with numerical results.

References

[1] L. Chen, Phys. Plasmas **1**, 1519, (1994).

[2] C.Z. Cheng, N.N. Gorelenkov and C.T. Hsu, Nucl. Fusion **35**, 1639, 1995.

[3] L.-J. Zheng and L. Chen, Phys. Plasmas **7**, 2469, (2000).

[4] R.A. Santoro and L. Chen, Phys. Plasmas **3**, 2349, (1996).

[5] S. Briguglio *et al.*, Phys. Plasmas **2**, 3711, (1995).

[6] S. Briguglio, F. Zonca and G. Vlad, Phys. Plasmas **5**, 3287, (1998).

[7] C.Z. Cheng, L. Chen and M.S. Chance, Ann. Phys. **161**, 21, (1985).

[8] R.R. Mett and S.M. Mahajan, Phys. Fluids B **4**, 2885, (1992).

[9] R.B. White *et al.*, Phys. Fluids **26**, 2958, (1983).

[10] W.W. Heidbrink, E.J. Strait, M.S. Chu and A.D. Turnbull, Phys. Rev. Lett. **71**, 855, (1993).

[11] F. Zonca and L. Chen, *Destabilization of Energetic Particle Modes by localized particle sources*, to be published on Phys. Plasmas (2000).

[12] F. Zonca, S. Briguglio, G. Fogaccia and G. Vlad, *Radio Frequency Power in Plasmas*, S. Bernabei and F. Paoletti Eds., pp. 56-65, AIP (1999).

[13] L. Chen, Z. Lin, R.B. White and F. Zonca, *Nonlinear Zonal Dynamics of Drift and Drift-Alfvén Turbulences in Tokamak Plasmas*, paper TH4/5, presented at this Conference.

[14] F. Zonca, S. Briguglio, L. Chen, G. Fogaccia and G. Vlad, *Theoretical Aspects of Collective Mode Excitations by Energetic Ions in Tokamaks*, to appear in the Proceedings of the Varenna-Lausanne Intl. Workshop, Varenna, Aug. 28.th - Sep. 1.st 2000.

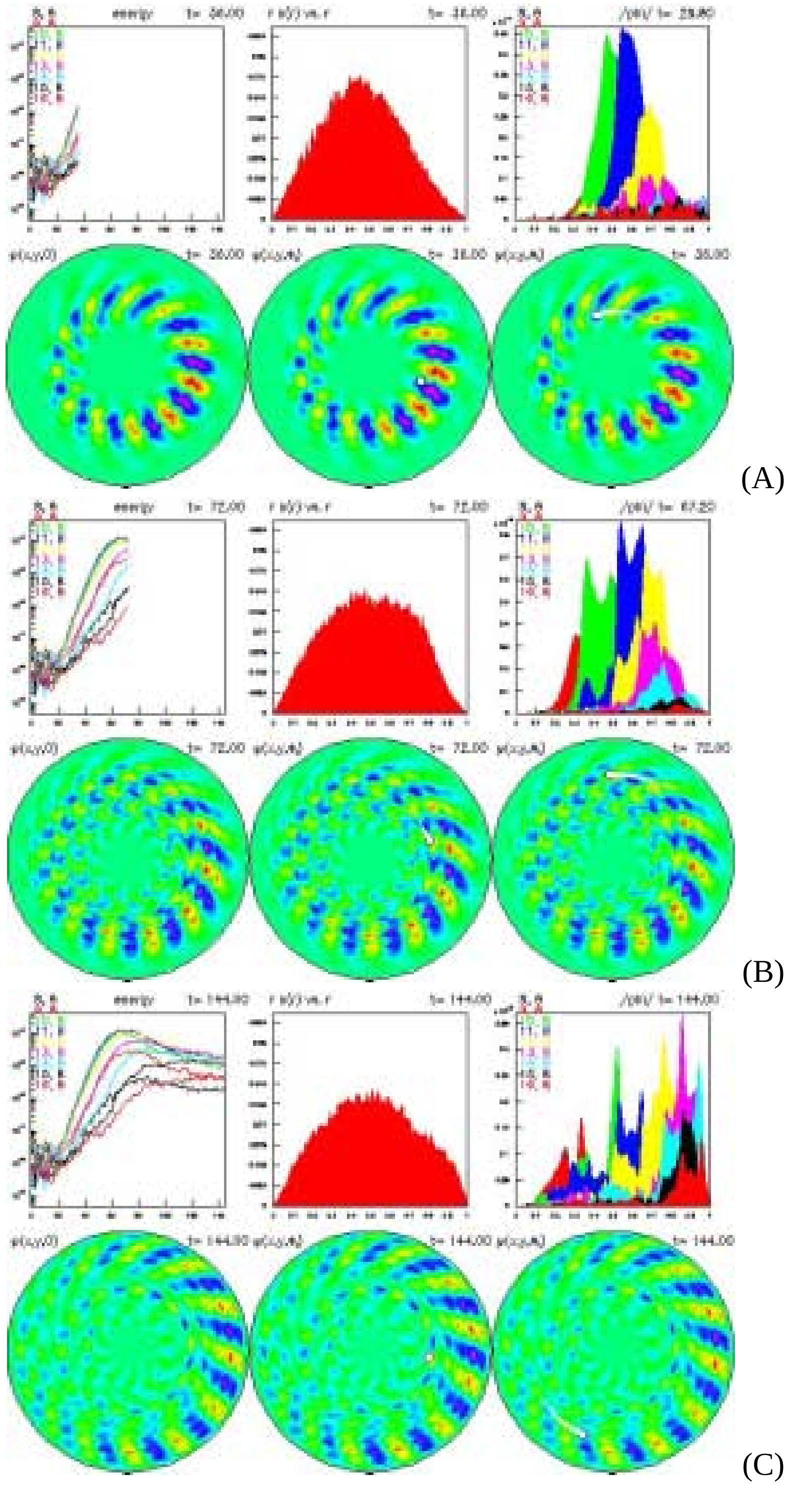

FIG. 2. : Nonlinear evolution of an $n = 8$ EPM at $t = 36R_0/v_A$ (A), $t = 72R_0/v_A$ (B) and $t = 144R_0/v_A$ (C). In each figure, six frames are visible. On the first row, from the left to the right: the wave energy in each poloidal component, the line density $rn_E(r)$ of energetic ions, and the radial mode structure. On the second row: the contour plot for the scalar potential fluctuation in the laboratory frame and at, respectively, the toroidal angles of a magnetically trapped and of a circulating particle (white bullet).